Arch Toxicol (2017) 91:1293–1307
DOI 10.1007/s00204-016-1775-y

MOLECULAR TOXICOLOGY

Activation of the Nrf2 signaling pathway in usnic acid-induced toxicity in HepG2 cells

Si Chen[1] · Zhuhong Zhang[2,3] · Tao Qing[4] · Zhen Ren[1] · Dianke Yu[5] · Letha Couch[1] · Baitang Ning[5] · Nan Mei[2] · Leming Shi[4] · William H. Tolleson[1] · Lei Guo[1]

Received: 23 March 2016 / Accepted: 20 June 2016 / Published online: 1 July 2016

Abstract Many usnic acid-containing dietary supplements have been marketed as weight loss agents, although severe hepatotoxicity and acute liver failure have been associated with their overuse. Our previous mechanistic studies revealed that autophagy, disturbance of calcium homeostasis, and ER stress are involved in usnic acid-induced toxicity. In this study, we investigated the role of oxidative stress and the Nrf2 signaling pathway in usnic acid-induced toxicity in HepG2 cells. We found that a 24-h treatment with usnic acid caused DNA damage and S-phase cell cycle arrest in a concentration-dependent manner. Usnic acid also triggered oxidative stress as demonstrated by increased reactive oxygen species generation and glutathione depletion. Short-term treatment (6 h) with usnic acid significantly increased the protein level for Nrf2 (nuclear factor erythroid 2-related factor 2), promoted Nrf2 translocation to the nucleus, up-regulated antioxidant response element (ARE)-luciferase reporter activity, and induced the expression of Nrf2-regulated targets, including glutathione reductase, glutathione S-transferase, and NAD(P)H quinone oxidoreductase-1 (NQO1). Furthermore, knockdown of Nrf2 with shRNA potentiated usnic acid-induced DNA damage and cytotoxicity. Taken together, our results show that usnic acid causes cell cycle dysregulation, DNA damage, and oxidative stress and that the Nrf2 signaling pathway is activated in usnic acid-induced cytotoxicity.

Keywords Usnic acid · Liver toxicity · Oxidative stress · Nrf2 pathway

Disclaimer This article is not an official guidance or policy statement of the U.S. FDA. No official support or endorsement by the U.S. FDA is intended or should be inferred.

✉ Lei Guo
lei.guo@fda.hhs.gov

1 Division of Biochemical Toxicology, National Center for Toxicological Research (NCTR)/U.S. Food and Drug Administration (FDA), HFT-110, 3900 NCTR Road, Jefferson, AR 72079, USA

2 Division of Genetic and Molecular Toxicology, National Center for Toxicological Research/U.S. FDA, Jefferson, AR 72079, USA

3 Tianjin Medical University General Hospital, Tianjin 300052, China

4 School of Pharmacy, School of Life Sciences, Fudan-Zhangjiang Center for Clinical Genomics and Zhanjiang Center for Translational Medicine, Fudan University, Shanghai 200438, China

5 Division of Systems Biology, National Center for Toxicological Research/U.S. FDA, Jefferson, AR 72079, USA

Introduction

Usnic acid is one of the most pharmacologically important constituents produced by *Usnea* lichens. Its antimicrobial, antiprotozoal, antiviral, anti-inflammatory and photoprotective activities have led to the wide clinical use of usnic acid-containing products as alternative medicines (Araujo et al. 2015; Guo et al. 2008). Besides applications in traditional medicine, usnic acid extracts and pure usnic acid have been taken as dietary supplements to stimulate weight loss. However, over 30 cases of acute liver failure (some severe cases even required liver transplantation) have been reported due to the use of relatively high doses of usnic acid that are required to produce significant weight reduction in some individuals (Durazo et al. 2004; Favreau et al. 2002; Neff et al. 2004; Yellapu et al. 2011). Despite the fact that the U.S. FDA has posted warnings on dietary

supplements that include usnic acid (CFSAN 2001), usnic acid-containing products are still available on the US market and the European market as well. A better understanding is needed of cellular mechanisms of usnic acid-induced toxicity due to the continued use or over-use of weight loss products containing this agent.

Reactive oxygen species (ROS), such as hydrogen peroxide (H_2O_2), lipid hydroperoxides (ROOH), superoxide ($\cdot O_2^-$), hydroxyl radical ($\cdot$OH), and singlet oxygen ($^1O_2$), are natural byproducts of normal cellular oxidative metabolism (Devasagayam et al. 2004; Doi et al. 2002; Ravanat et al. 2004). In biological systems, a complex network of antioxidant substances provides an antioxidant defensive system to suppress the damaging effects of excess ROS (Vertuani et al. 2004). Certain stressed conditions can induce accumulation of ROS due to insufficient levels of antioxidants and/or the inhibition of protective antioxidant enzyme systems. These changes can disrupt the balance between the production of ROS and antioxidative defenses, resulting in oxidative stress and cellular damage (Sies 1997). Subsequently, disproportionate oxidative stress causes dysregulation of cell cycle progression (Shackelford et al. 2000), DNA strand breaks (Evans and Cooke 2004), apoptosis (Ozben 2007), and eventually cell death (Martindale and Holbrook 2002).

A key element in the regulation of antioxidant defensive systems is the activation of the Nrf2 (nuclear factor erythroid 2-related factor 2)–ARE (antioxidant response element) signaling pathway (Bryan et al. 2013; Nguyen et al. 2009). Nrf2 is a transcription factor that regulates the expression of numerous antioxidant proteins, including NAD(P)H quinone oxidoreductase-1 (NQO1) (Venugopal and Jaiswal 1996), γ-glutamate-cysteine synthetase (γ-GCSc) (Solis et al. 2002), heme oxygenase-1 (HO-1) (Alam et al. 1999), glutathione S-transferase (GST) (Hayes et al. 2000), and glutathione reductase (Thimmulappa et al. 2002). Under normal conditions, Nrf2 is degraded dynamically by the ubiquitin–proteasome system, keeping the expression of its downstream genes at low basal levels. Upon exposure to stress signals, the rate of Nrf2 degradation decreases, while the activation and accumulation of Nrf2 increase, which stimulates the expression of target antioxidant enzyme systems that provide protection against stress-induced cell death (Nguyen et al. 2009).

Our previous studies demonstrated that usnic acid disturbs cell cycle progression and induces apoptosis in HepG2 cells (Chen et al. 2014a). Usnic acid treatment increased ROS generation in both HepG2 cells and mouse primary hepatocytes, which was detected using the cell permeable redox-sensitive fluorescent dyes dihydrodichlorofluorescein diacetate and CellROX Green (Han et al. 2004; Sahu et al. 2012). In our gene expression study, HepG2 cells were exposed to usnic acid at various concentrations for 2, 6, or 24 h and then subjected to RNA-sequencing analysis (RNA-seq) to understand better the cell signaling pathways affected by usnic acid. Pathway analysis indicated that the NRF2-mediated Oxidative Stress Response may be important in usnic acid's toxicity. These results stimulated the current investigation to determine if oxidative stress is a possible mechanism contributing to usnic acid-induced liver toxicity. Therefore, we evaluated the production of ROS and its biological effects using various biological approaches. We also investigated the role of the Nrf2–ARE signaling pathway in the cytotoxicity of usnic acid. We demonstrated that the Nrf2-dependent adaptive defense response was activated during exposure to usnic acid for 6 h, while S-phase cell cycle arrest, DNA damage, accumulation of ROS, and glutathione depletion were induced with prolonged (24 h) treatment in HepG2 cells. We also studied the direct involvement of Nrf2 in usnic acid-induced cytotoxicity by silencing the expression of the Nrf2 gene. Our data indicate that activation of Nrf2 signaling pathway is important in usnic acid-induced DNA damage and cytotoxicity.

Materials and methods

Chemicals and reagents

Usnic acid, dimethyl sulfoxide (DMSO), Williams' medium E, Dulbecco's modified Eagle's medium (DMEM), *N*-acetyl-L-cysteine (NAC), and propidium iodide were from Sigma-Aldrich (St. Louis, MO). Fetal bovine serum (FBS) was obtained from Atlanta Biologicals (Lawrenceville, GA). Antibiotic–antimycotic, puromycin, 2′,7′-dichlorodihydrofluorescein diacetate (H_2DCFDA), and CellROX® Green reagent were from Life Technologies (Grand Island, NY). RNase A was from Qiagen (Valencia, CA). For Western blotting assays, the primary antibodies against the cyclins D1 and D3, cyclin-dependent kinases 2, 4, and 6 (CDK2, CDK4, and CDK6), activated checkpoint kinases 1 and 2 (phospho-CHK1(phospho-Ser345), phospho-CHK2 (phospho-Thr68)), gamma-histone 2AX (γ-H2A.X (phospho-Ser139)), heme oxygenase-1 (HO-1), and NAD(P)H quinone oxidoreductase-1 (NQO1) were purchased from Cell Signaling Technology (Danvers, MA). Antibodies for glutathione S-transferase alpha (ab135709) were obtained from Abcam (Cambridge, MA). Antibodies for γ-GCSc, Nrf2, glutathione reductase, GAPDH, and lamin B1 were purchased from Santa Cruz Biotechnology (Santa Cruz, CA).

Cell culture and treatment with usnic acid

The HepG2 human hepatoma cell line was purchased from the American Type Culture Collection (ATCC; Manassas,

VA). HepG2 cells were cultured in Williams' medium E supplemented with 10 % FBS and 100 units/ml of penicillin, 100 µg/ml of streptomycin, and 0.25 µg/ml of Fungizone® Antimycotic at 37 °C in a humidified atmosphere with 5 % CO_2. The passage number did not exceed 10. Usnic acid working solutions (1000×) were freshly prepared prior to use by dissolving usnic acid in DMSO. Cells were seeded at a density of 3×10^5/ml cells in 96-well plates, 60-mm, or 100-mm tissue culture dishes. Cells were cultured for 24 h prior to treatment with usnic acid or the DMSO vehicle control. The final concentration of DMSO was 0.1 %.

Cell cycle analysis

The sub-diploid DNA peaks and cell cycle distribution of the HepG2 cells were measured using flow cytometry-based cell cycle analysis as described previously (Chen et al. 2014a).

Alkaline comet assay

Alkaline comet assays were conducted as described previously (Zhang et al. 2015). Briefly, HepG2 cells were seeded into 6-well plates and incubated overnight. The cells were exposed to two-fold serial dilutions of usnic acid (3.13–50 µM) for 24 h. After exposure, the DNA single- and double-strand breaks created in the treated cells were measured using the CometAssay® reagent kit for single-cell gel electrophoresis assays (Trevigen, Gaithersburg, MD). Three slides were used for each concentration and a total of 100 cells per slide were scored. The percentage of DNA in tails was calculated as the DNA damage parameter.

Measurement of ROS

Intracellular ROS production was measured using fluorescent staining using the redox-sensitive dyes H_2DCFDA and CellROX® Green reagent. HepG2 cells seeded in 96-well plates were stained with 10 µM H_2DCFDA. Following incubation for 30 min at 37 °C in the dark, cells were washed with PBS to remove unincorporated dye. Cells were then exposed to usnic acid at concentrations from 3.13 to 50 µM in phenol red-free medium. The cells were continuously incubated at 37 °C with 5 % CO_2, and the fluorescence intensities were measured at 10, 30 min, 1-, 2-, 4-, 6-, and 24-h time points with a Synergy H4 microplate reader (BioTek, Winooski, VT).

CellROX Green® assays were conducted according to the manufacturer's protocols. Briefly, HepG2 cells seeded in 96-well plates were treated with usnic acid for 2 and 6 h, and then, 5 µM CellROX Green® reagent was added to the cells and incubated for 30 min at 37 °C. After cells were washed with PBS, the fluorescence intensities were determined with a Synergy H4 microplate reader. Background fluorescence signals, determined in a set of cell-free wells, were subtracted from sample signals.

Measurement of glutathione levels

Total intracellular glutathione (GSH) levels of HepG2 cells were measured after usnic acid treatment for 24 h using HT glutathione assay kit (Trevigen). The data were normalized against total protein content as determined by a Bio-Rad protein assay (Bio-Rad, Hercules, CA). The GSH/oxidized glutathione (GSSG) ratios in usnic acid-treated cells were determined using GSH/GSSG-Glo assay kit (Promega) as described by the manufacturer.

RNA isolation and quantitative real-time PCR

Total RNA was isolated using a RNeasy mini kit (Qiagen, Valencia, CA). cDNA was synthesized from 2 µg of total RNA using a high-capacity cDNA reverse transcription kit (Applied Biosystems, Foster City, CA) according to the manufacturer's protocol. Real-time PCR was performed as described previously (Chen et al. 2014b) to examine the gene expression levels of Nrf2 and GAPDH using the following probes obtained from Applied Biosystems: human Nrf2 (NFE2L2, Hs00975961_g1) and human GAPDH (Hs02758991_g1).

Antioxidant response dual-luciferase reporter assay

A Cignal Antioxidant Response dual-luciferase assay (Qiagen) was used to assess the activation of the Nrf2/Nrf1 signal-transduction pathway in usnic acid-treated HepG2 cells. The assay was performed according to the manufacturer's protocol (G. transfection and treatment protocol for reporter assay + peptide/recombinant protein). Briefly, HepG2 cells at a density of 3×10^4 cells per well were reverse transfected with Cignal reporter, Cignal negative control, or Cignal positive control plasmids using Lipofectamine® 2000 Transfection Reagent (Thermo Fisher Scientific, Waltham, MA). After transfection and recovery for 24 h, cells in 6 replicate wells were treated with various concentrations of usnic acid for an additional 6 h. *Firefly* and *Renilla* luciferase activities were determined using a Dual-Luciferase® Reporter Assay System (Promega Corporation, Madison, WI).

Vector construction and stable cell lines establishment

The 293T cell line used for lentivirus packaging was obtained from Biosettia (San Diego, CA) and maintained in DMEM supplemented with 10 % FBS, 1 mM sodium pyruvate and 0.1 mM nonessential amino acids.

A specific target site for silencing of human Nrf2 was identified using the shRNA Designer software available at Biosettia's website (http://biosettia.com/support/shrna-designer/). Small hairpin RNA (shRNA) sequences were designed for insertion into a doxycycline (DOX)-inducible shRNA lentiviral expression vector pLV-H1tetO-GFP-Puro (Biosettia). The following shRNA-encoding DNA oligonucleotides containing inner palindromic sequences were synthesized (Biosynthesis, Inc., Lewisville, Texas): sh-Nrf2 (5′- AAAAGCCCATTGATGTTTCT GATTTGGATCCAAATCAGAAACATCAATGGGC-3′) and the scramble shRNA (5′-AAAAGCTACACTATC GAGCAATTTTGGATCCAAAATTGCTCGATAGTG TAGC-3′). The scramble shRNA sequence does not contain significant homology to known genes and was used as a negative control in silencing experiments. The generation of the lentiviral shRNA vectors and the establishment of the stable HepG2 cell line derivatives were described previously (Chen et al. 2014a). In total, two stable cell lines were generated, namely SC (scramble control) and sh-Nrf2.

Cellular ATP level measurement

ATP content was quantified using a CellTiter-Glo luminescent cell viability assay (Promega) according to the manufacturer's instructions. The cellular ATP content was calculated by comparing the intensities of luminescence of the treated cells to that of the DMSO vehicle controls.

Western blot analysis

Cells were cultured in 60- or 100-mm tissue culture plates and treated with usnic acid. After 6 or 24 h of usnic acid treatment, whole-cell lysates were prepared using RIPA buffer containing Halt Protease Inhibitor Cocktail (Thermo Fisher Scientific). The extraction of separate cytoplasmic and nuclear protein fractions was performed using a NE-PER™ nuclear and cytoplasmic extraction reagents kit (Thermo Fisher Scientific) according to the manufacturer's instructions. The concentrations of the protein samples were determined using a Bio-Rad protein assay (Bio-Rad Laboratories, Hercules, CA). Standard Western blots were performed. Depending on the proteins of interest in different blots, antibodies were selected from among those against cyclin D1, cyclin D3, CDK2, CDK4, CDK6, phospho-CHK1 (Ser345), phospho-CHK2 (Thr68), γ-H2A.x (Ser139), HO-1, NQO1, glutathione S-transferase alpha, γ-GCSc, Nrf2, and glutathione reductase followed by an incubation with secondary antibody conjugated with horseradish peroxidase (HRP) (Santa Cruz Biotechnology). GAPDH and lamin B1 were used as internal controls. The protein signals were determined and quantified with a FluorChem E System (ProteinSimple, San Jose, CA).

RNA-seq analysis

RNA-seq gene expression analysis was performed at the Microarray Core Facility of the University of Texas Southwestern Medical Center (http://microarray.swmed.edu). RNA-Seq libraries were constructed and sequenced using the TruSeq protocol on an Illumina HiSeq 2000 platform. The low-quality reads were removed by Trimmomatic v 0.32 (Bolger et al. 2014). Human genome Ensembl GRCh37, downloaded from (http://ftp.ensembl.org/pub/release-75//fasta/homo_sapiens/dna/), was used as the reference genome and gene annotation, with 52,369 genes included. High-quality reads were aligned to the reference genome using TopHat v 2.0.8b (Trapnell et al. 2012), allowing a maximum number of 2 mismatches. Cufflinks v 2.0.2 was used for gene quantification (Trapnell et al. 2012). The default parameter settings were used. For each sample, read counts were normalized as reads per million mapped reads (RPM) and then transformed to $\log_2$ scale. To avoid infinite values, a value of one was added to each gene count before $\log_2$ transformation. In this study, a differentially expressed gene (DEG) was identified with a fold change (FC) greater than 1.5 (up or down) and a nonstringent p cutoff of 0.05 in comparison with the control group. Principal component analysis (PCA) and Student's t test were performed using functions "prcomp" and "t.test" in the "stats" package of R project.

Statistical analyses

Data are presented as the mean ± standard deviation (SD) of at least three independent experiments. Analyses were performed using GraphPad Prism 5 (GraphPad Software, San Diego, CA). Statistical significance was determined by one-way analysis of variance (ANOVA) followed by the Dunnett's tests for pairwise-comparisons or two-way ANOVA followed by the Bonferroni post test. The difference was considered statistically significant when p was less than 0.05.

Results

Analysis of differentially expressed genes

To identify signaling pathways of usnic acid-induced hepatotoxicity, HepG2 cells were treated with usnic acid and then RNA was isolated and gene expression profiles were determined by RNA sequencing. There were three treatment groups (3.13, 12.5, and 50 μM) and one DMSO control group, each group containing four biological replicates, and the treatments were performed for three time points (2, 6, and 24 h). A total of 48 RNA samples were subjected to RNA-seq, and the sequencing was done in triplicate (i.e.,

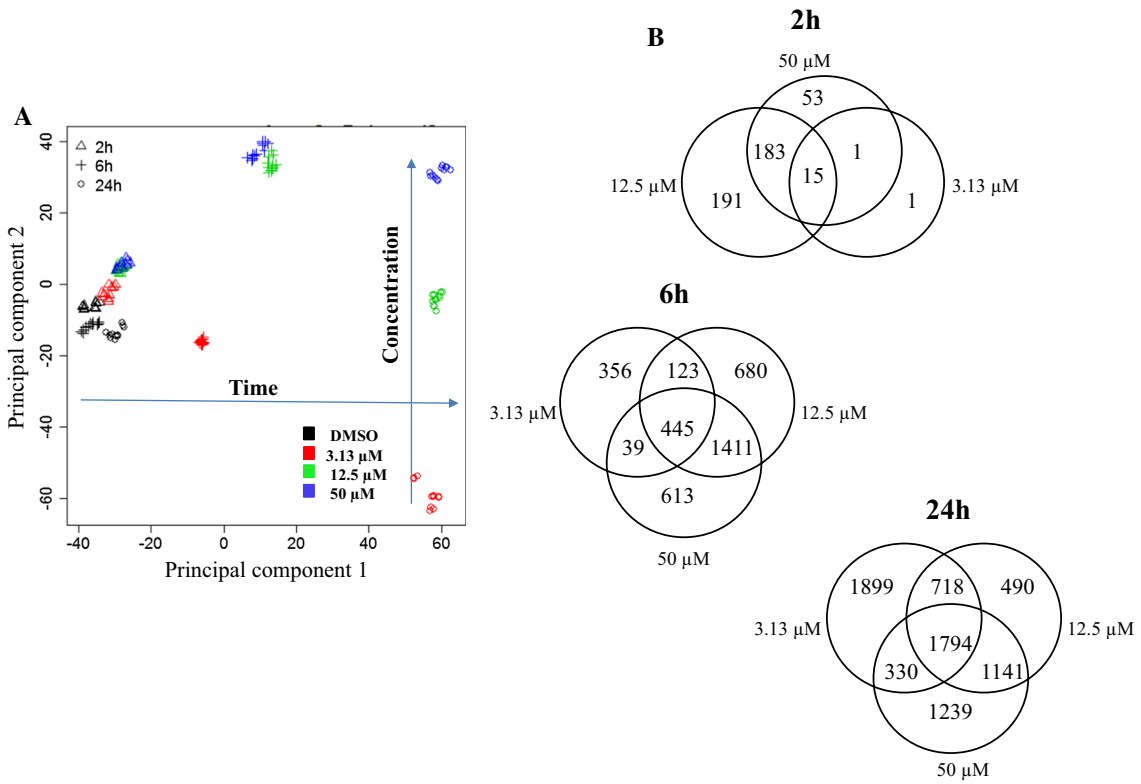

Fig. 1 **a** Principal component analysis (PCA) of gene expression profiles. The values of the $\log_2$ (RPM) of genes were used for PCA analysis. The intensity of the entire gene set was used; no specific cut off was applied for the analysis. **b** Numbers of differentially expressed genes. A gene was identified as differentially expressed if the fold change >1.5 (up or down) and the *p* value <0.05 in comparison with the control group

on three lanes) for each RNA sample; thus, a total of 144 files were generated. To explore the treatment effect and to determine the relationship of the samples based on expression profiles, unsupervised principal component analysis (PCA) was performed for the entire gene set and the PCA result is displayed in Fig. 1a. Samples are grouped primarily according to the time points and then separated by the treatment groups; especially, a clear separation according to the concentration was observed at 24-h treatment. A differentially expressed gene was defined when a fold change is larger than 1.5 (up or down) and a FDR adjusted *t* test *p* value <0.05 in comparison with the DMSO control group. As displayed in the Venn diagrams (Fig. 1b), large numbers of differentially expressed genes in the groups receiving 12.5 µM usnic acid are overlapped with the higher-concentration groups (50 µM) for all three time points; therefore, further analysis was focused on 12.5 µM treatment groups. Biological process and pathway analysis were performed using ingenuity pathway analysis (IPA). The top 20 pathways identified are listed in Table 1. Interestingly, ROS, cell cycle, and DNA damage related pathways such as "Role of BRCA1 in DNA Damage Response," "GADD45 Signaling," "DNA Double-Strand Break Repair," "ATM Signaling," "Cell Cycle: G2/M DNA Damage Checkpoint Regulation," and "NRF2-mediated Oxidative Stress Response" were identified and some of them are overlapped in three time points. These results prompted us to verify the findings by gene expression analysis and to study the possible roles of some of these pathways.

Usnic acid induces S-phase cell cycle arrest

In agreement with pathway analysis result in which cell cycle is possibly perturbed, we found that usnic acid induced a significant increase in the proportion of cells in S phase, accompanied by a concordant decrease in the proportion of cells in G0/G1 and G2/M phases as indicated in Fig. 2a. Cyclin D–cyclin-dependent kinase (CDK) 2 and CDK 4/6-cyclin D1/D3 complex accumulation are important for cell cycle progression through the S phase (Bertoli et al. 2013). As shown in Fig. 2b, c, treatment with usnic acid for 24 h markedly decreased CDK2, CDK4, CDK6, cyclin D1, and cyclin D3 expression levels in a concentration-dependent manner.

The S phase of the cell cycle is the period in which DNA is replicated and has a DNA content intermediate between

Table 1 Top 20 canonical pathways altered by usnic acid

	Pathway	*p* value
12.5 μM usnic acid/2 h		
1	Hepatic fibrosis/hepatic stellate cell activation	1.62E−08
2	IL-17A signaling in gastric cells	4.07E−07
3	TNFR2 signaling	1.05E−06
4	Role of IL-17A in psoriasis	1.32E−05
5	Glucocorticoid receptor signaling	1.70E−05
6	TNFR1 signaling	2.57E−05
7	Neuregulin signaling	9.12E−05
8	Airway pathology in chronic obstructive pulmonary disease	9.12E−05
9	HMGB1 signaling	1.00E−04
10	Toll-like receptor signaling	2.63E−04
11	Aryl hydrocarbon receptor signaling	2.95E−04
12	Production of nitric oxide and reactive oxygen species	3.31E−04
13	ILK signaling	4.27E−04
14	Role of IL-17A in arthritis	4.68E−04
15	IL-6 signaling	5.01E−04
16	ATM signaling	7.08E−04
17	IL-17A signaling in fibroblasts	7.94E−04
18	PPAR signaling	9.55E−04
19	GADD45 signaling	1.45E−03
20	NRF2-mediated oxidative stress response	1.51E−03
12.5 μM usnic acid/6 h		
1	Role of BRCA1 in DNA damage response	9.33E−05
2	GADD45 signaling	1.95E−04
3	Death receptor signaling	2.69E−04
4	Mismatch repair in eukaryotes	2.82E−04
5	Mouse embryonic stem cell pluripotency	4.57E−04
6	TWEAK signaling	5.13E−04
7	TNFR1 signaling	6.17E−04
8	ILK signaling	1.26E−03
9	Hereditary breast cancer signaling	1.62E−03
10	Cell cycle: G1/S checkpoint regulation	1.62E−03
11	Factors promoting cardiogenesis in vertebrates	1.66E−03
12	TNFR2 signaling	1.82E−03
13	Molecular mechanisms of cancer	2.63E−03
14	Aldosterone signaling in epithelial cells	3.47E−03
15	Colorectal cancer metastasis signaling	3.63E−03
16	Activation of IRF by cytosolic pattern recognition receptors	4.27E−03
17	DNA double-strand break repair	4.47E−03
18	ATM signaling	4.68E−03
19	Cell cycle: G2/M DNA damage checkpoint regulation	5.62E−03
20	Mitotic roles of polo-like kinase	5.89E−03
12.5 μM usnic acid/24 h		
1	LPS/IL-1 mediated inhibition of RXR function	5.62E−08
2	FXR/RXR activation	6.46E−07
3	NRF2-mediated oxidative stress response	1.05E−06
4	Xenobiotic metabolism signaling	2.00E−05
5	Acute phase response signaling	2.51E−05
6	Role of macrophages, fibroblasts, and endothelial cells	2.82E−05
7	Aldosterone signaling in epithelial cells	3.89E−05
8	Growth hormone signaling	5.37E−05
9	Prolactin signaling	6.31E−05
10	Glycine betaine degradation	6.92E−05
11	Aryl hydrocarbon receptor signaling	7.59E−05
12	Superpathway of cholesterol biosynthesis	1.17E−04
13	p53 signaling	1.55E−04
14	Type II diabetes mellitus signaling	3.55E−04
15	Thrombopoietin signaling	4.17E−04
16	Coagulation system	4.37E−04
17	PXR/RXR activation	6.17E−04
18	LXR/RXR activation	7.41E−04
19	eNOS signaling	7.59E−04
20	VEGF family ligand–receptor interactions	9.12E−04

that of cells in G0/G1 phase and G2/M phase (Bell and Dutta 2002). Increased accumulation in S phase could be attributed to an increase in cells that are actively replicating DNA; however, this may not be the case for usnic acid treatment. Our previous report showed that usnic acid inhibited cell proliferation (Chen et al. 2014a), and our current results show that usnic acid reduces the expression of key cyclin-related proteins that are critical for S phase progression, as indicated in Fig. 2. Collectively, our data suggest that the increase in the number of cells in S phase following usnic acid treatment is more likely due to cell cycle arrest.

Usnic acid causes DNA damage

It has been reported that S-phase arrest may be accompanied by DNA damage and S-phase checkpoint activation (Yang et al. 2014; Ye et al. 2003); therefore, we examined whether or not usnic acid induces DNA damage using a single-cell gel electrophoresis assay, also referred to as the comet assay. HepG2 cells exposed to usnic acid for 24 h exhibited a concentration-dependent increase in comet tail intensities (Fig. 3a). Significant DNA damage was observed at concentrations as low as 6.25 μM with 15.4 % of tail intensity, whereas 8 % of tail intensity appeared in DMSO vehicle control cells. The presence of DNA strand breaks was confirmed by measuring histone H2A.X phosphorylation at serine 139 (γ-H2A.X), a hallmark of DNA double-strand breakage in cells (Rogakou et al. 1998). Consistent with the results from

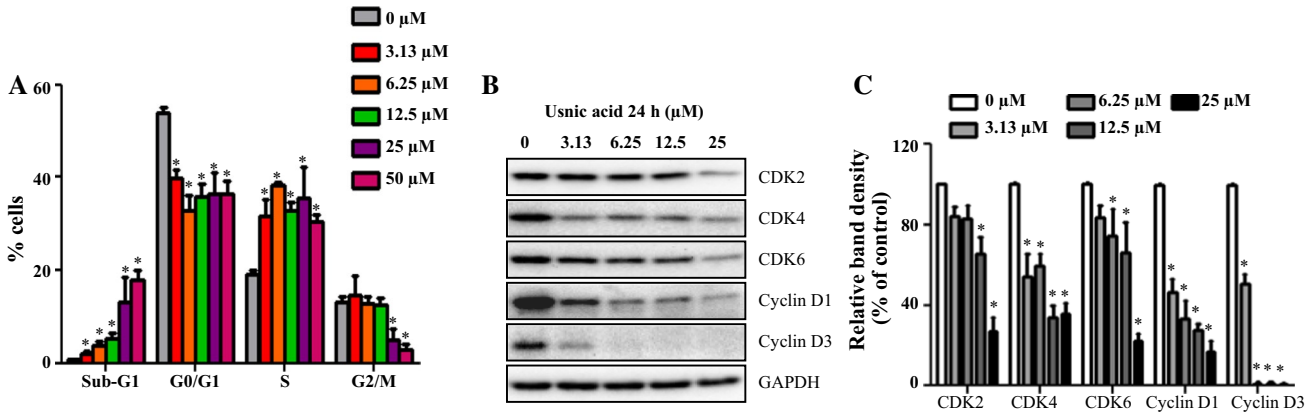

Fig. 2 Usnic acid induces S-phase cell cycle arrest in HepG2 cells. HepG2 cells were exposed to 3.13, 6.25, 12.5, 25, and 50 μM usnic acid for 24 h, with DMSO as the vehicle control. **a** Cell cycle was assessed using flow cytometry. The *bar graph* depicts the mean percentage of each cell cycle phase ± SD from four independent experiments. *$p < 0.05$ compared with the control for each cell cycle phase. **b**, **c** The expression of S-phase progression-related proteins was determined. HepG2 cells were treated with the indicated concentrations of usnic acid for 24 h. Treated cells were lysed and subjected to Western blotting with antibodies against CDK2, CDK4, CDK6, Cyclin D1, and Cyclin D3. GAPDH was used as a loading control. Intensities of bands were normalized to the amount of GAPDH. *$p < 0.05$ versus treatment of DMSO vehicle control

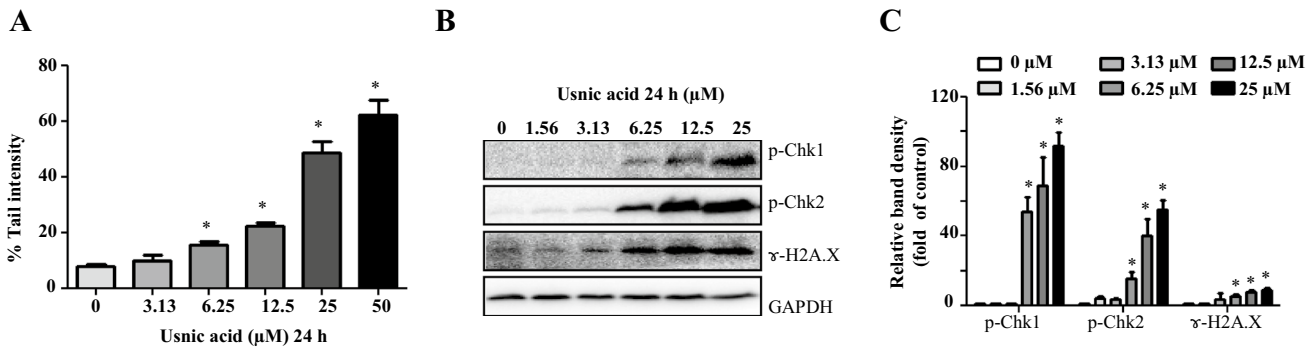

Fig. 3 Usnic acid causes DNA damage in HepG2 cells. HepG2 cells were treated with the indicated concentrations of usnic acid for 24 h. **a** Quantification of the percentages of cells with comet tails at different concentrations. Data are the mean ± SD ($n = 100$ cells in each of three trials; *$p < 0.05$ compared with DMSO vehicle control). **b**, **c** Total cellular proteins were extracted, and the levels of phosphorylated-Chk1, phosphorylated-Chk2, and γ-H2A.X were measured. GAPDH was used as a loading control. Intensities of bands were normalized to the amount of GAPDH. *$p < 0.05$ versus treatment of DMSO vehicle control

the comet assay, starting at 6.25 μM, treatment of HepG2 cells with usnic acid for 24 h displayed concentration-dependent upregulation of γ-H2A.X along with the induction of two cell cycle checkpoint-related proteins, phosphorylated-Chk1 (p-Chk1) and phosphorylated-Chk2 (p-Chk2) (Fig. 3b, c).

Usnic acid triggers ROS generation

DNA damage can result from ROS accumulation; thus, ROS generation was examined. We evaluated intracellular ROS levels in HepG2 cells treated with usnic acid using two redox-sensitive dyes, H_2DCFDA and CellROX Green. The results with H_2DCFDA staining showed that usnic acid induced time- and concentration-dependent increases in ROS levels (Fig. 4a). ROS levels increased significantly as early as 10 min after treatment with 6.25 μM usnic acid. The increased production of ROS was confirmed using another fluorescent indicator of oxidative stress, CellROX® Green reagent. As shown in Fig. 4b, significantly increased ROS levels in response to usnic acid exposure were confirmed using CellROX Green staining.

Usnic acid depletes glutathione

In general, an elevated level of ROS is a major indicator of oxidative stress (Sies 1997). To determine whether or not usnic acid induces oxidative stress in response to increase ROS levels, we first examined the level of total

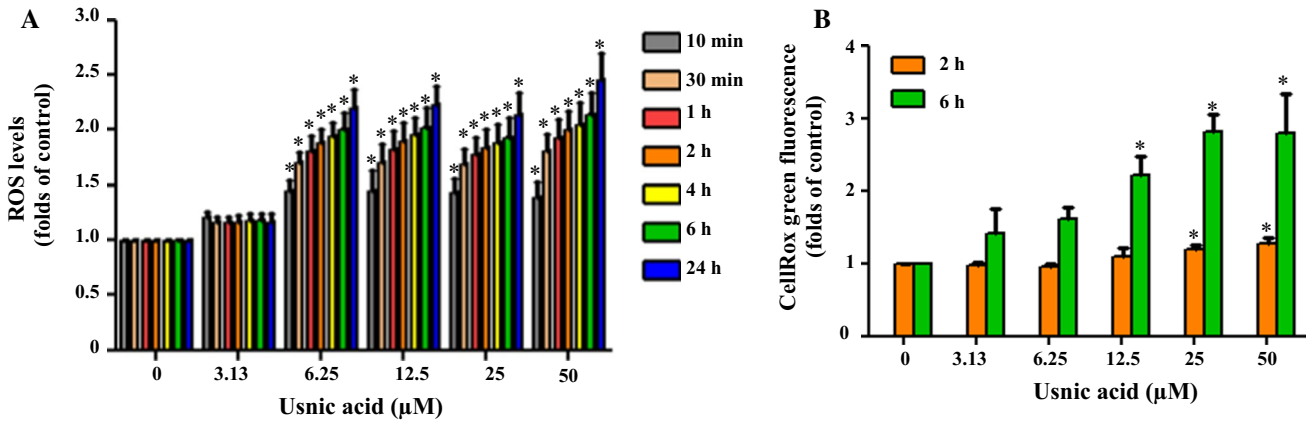

Fig. 4 Usnic acid triggers ROS generation in HepG2 cells. **a** The ROS values were measured at 10 and 30 min, and 1, 2, 4, 6, and 24 h after exposure to different concentrations of usnic acid by H_2DCFDA staining. **b** The ROS levels were further confirmed by CellROX® oxidative stress green fluorescence reagent at 2- and 6-h time points of usnic acid treatment. *Bar graphs* are mean ± SD of three individual experiments. *$p < 0.05$ versus treatment of DMSO vehicle control for each time point

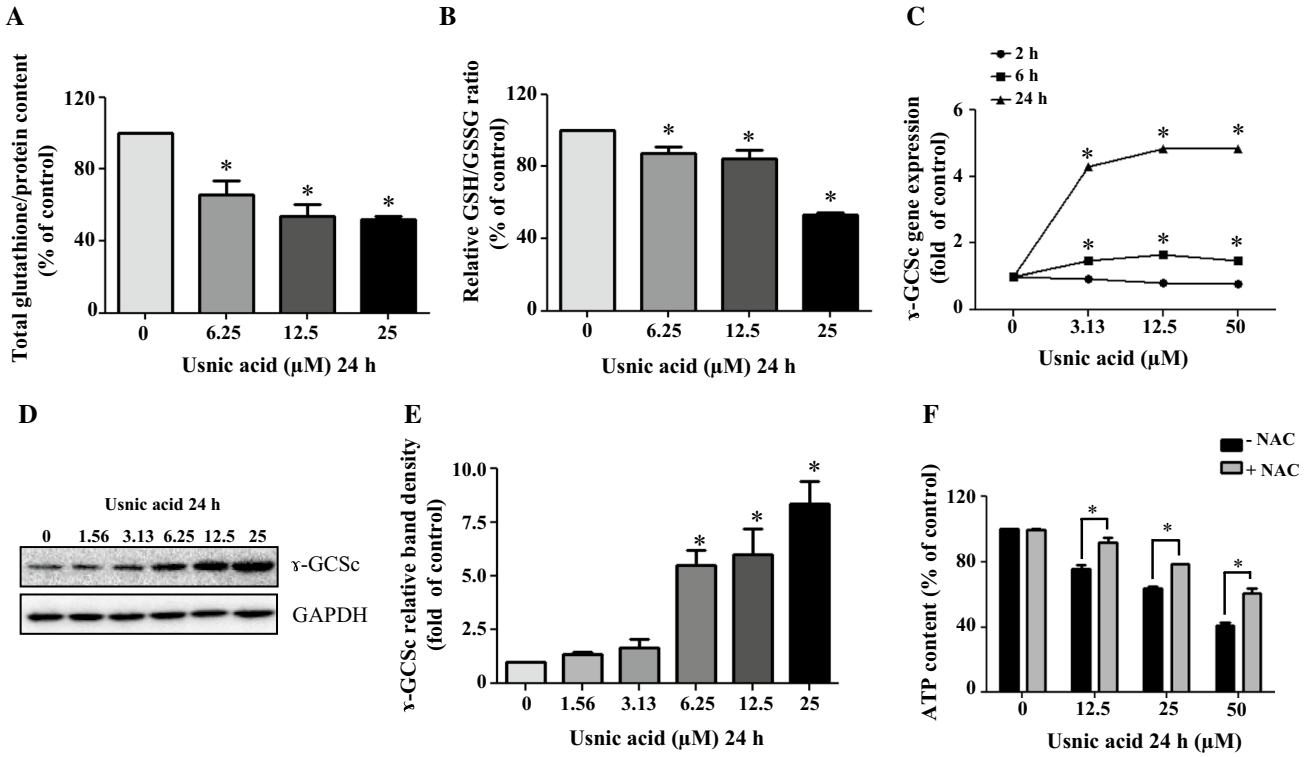

Fig. 5 Usnic acid induces oxidative stress in HepG2 cells. **a** Total intracellular glutathione levels were determined after a 24-h usnic acid treatment. The data were normalized against the total protein content as determined by Bio-Rad protein assay. **b** GSH/GSSG ratios were measured and calculated after 24 h of usnic acid treatment. **c** The gene expression levels of γ-GCSc were measured by RNA-seq. **d**, **e** Total cellular proteins were extracted, and the levels of γ-GCSc were detected by Western blotting. GAPDH was used as a loading control. Intensities of bands of γ-GCSc were normalized to the amount of GAPDH. **f** HepG2 cell were pretreated with 10 mM NAC for 1 h then treated with usnic acid for additional 24 h with 2.5 mM NAC remained in the medium. Cell viability was determined by ATP content. *Bar graphs* are mean ± SD of three individual experiments. *$p < 0.05$ compared with DMSO vehicle control

and reduced form of glutathione, a key antioxidant, in usnic acid-treated HepG2 cells. The total glutathione level was decreased markedly in cells exposed to usnic acid for 24 h (Fig. 5a). Besides the depletion of total glutathione content, ratios of glutathione in its reduced form (GSH)/oxidized form (GSSG) were significantly decreased in cells treated

with 6.25–25 μM usnic acid for 24 h (Fig. 5b). Synthesis of the enzyme γ-GCSc is the first and rate-limiting step in the *de novo* synthesis of cellular glutathione (Solis et al. 2002); γ-GCSc expression can be induced to compensate for exhaustive GSH depletion and prevent oxidative stress. Our RNA-seq result indicates that there was time- and concentration-dependent increase in gene expression of γ-GCSc, and more than 4 times induction was observed with 24-h treatment (Fig. 5c). This gene expression result was further validated by Western blot analysis. As shown in Fig. 5d, e, treatment with 6.25–25 μM usnic acid resulted in significantly increased γ-GCSc protein expression levels, suggesting that γ-GCSc induction occurred at both transcriptional and translational levels. Furthermore, the effect of the ROS scavenger N-acetyl-L-cysteine (NAC) on usnic acid-induced cytotoxicity was evaluated. Cells were pretreated with 10 mM NAC for 1 h and then treated with usnic acid for additional 24 h in the presence of 2.5 mM NAC. As shown in Fig. 5f, NAC significantly attenuated usnic acid-induced ATP depletion. Collectively, these data demonstrated that oxidative stress was induced by usnic acid.

Usnic acid activates Nrf2–ARE antioxidant response signaling pathway

Nrf2, a basic leucine zipper transcription factor encoded by the NFE2L2 gene, plays a defensive role against oxidative insults by regulating the expression of downstream antioxidant proteins (Gold et al. 2012). γ-GCSc is a characteristic Nrf2 target gene, and usnic acid concentration-dependent upregulation of γ-GCSc was discovered in this study (Fig. 5c–e); thus, it was important to investigate the involvement of the Nrf2 signaling pathway in response to usnic acid-induced oxidative stress. Treatment with usnic acid significantly increased the expression of total Nrf2 at the protein level compared to the DMSO control (Fig. 6a, b). The Nrf2 expression levels in the cytosol and nucleus were also examined. As shown in Fig. 6a, b, exposure to usnic acid markedly increased the fraction of Nrf2 detected in the nucleus, accompanied by a decreased proportion in the cytosol, indicating that Nrf2 was translocated into the nucleus from the cytosol in response to usnic acid.

Once released into the nucleus, Nrf2 executes its transcriptional activity by binding to the antioxidant response elements (ARE) of downstream antioxidative genes and regulating their transcription (Itoh et al. 1997). We then determined whether or not usnic acid activates Nrf2-driven ARE activity using a dual-luciferase reporter assay. HepG2 cells were transfected with a plasmid encoding a luciferase reporter gene whose expression is driven by an ARE-containing promoter (ARE-luciferase) and then the cells were treated with usnic acid. Figure 6c shows that usnic acid treatment for 6 h significantly upregulated ARE-dependent luciferase reporter activity in a concentration-dependent fashion. We next examined the expression of Nrf2 downstream antioxidative enzymes using Western blot analysis. As displayed in Fig. 6d, e, usnic acid treatment for 6 h profoundly increased the levels of glutathione reductase and glutathione S-transferase and slightly increased NQO1, whereas there was no significant change in HO-1 expression levels. Taken together, these results indicate that treatment with usnic acid upregulates Nrf2 expression (Fig. 6a) and promotes Nrf2 translocation, resulting in activation of the Nrf2–ARE signaling pathway (Fig. 6c, d).

Nrf2 signaling pathway activation prevents usnic acid-induced cytotoxicity and DNA damage

To confirm further that the Nrf2 signaling pathway is involved in usnic acid-induced cytotoxicity, Nrf2, the key molecular regulator in this pathway, was silenced in HepG2 cells using a doxycycline-induced lentivirus system. The knockdown efficiency of sh-Nrf2 was analyzed by real-time PCR and Western blotting. As shown in Fig. 7a–c, sh-Nrf2 effectively silenced Nrf2 at both mRNA and protein levels with the efficiencies of 88 and 97 %, respectively. As expected, the increased expression of γ-GCSc in response to 25 μM usnic acid was markedly reduced by knockdown of Nrf2 compared with scramble control (Fig. 7d, e). Furthermore, we investigated the effect of Nrf2 on usnic acid-induced DNA damage. Figure 8a, b shows that Nrf2 silencing increased the extent of DNA damage caused by 25 μM usnic acid as indicated by the further induction of γ-H2A.X in comparison with the same treatment of scramble control cells. In addition, silencing Nrf2 significantly decreased cell viability compared with the scramble control cells treated with usnic acid (Fig. 8c). These data suggest that the Nrf2 signaling pathway is directly involved in usnic acid-induced cytotoxicity and DNA damage.

Discussion

Previously we have studied hepatic toxic effects of usnic acid using different in vitro systems, including HepG2 cells, rat primary hepatocytes, and human primary hepatocytes. Although different sensitivities were observed in distinct cells, we obtained similar toxicity results with multiple endpoints. Our mechanistic studies in HepG2 cells revealed that various signaling pathways were affected by usnic acid (Chen et al. 2014a, 2015). In this study, we continued to use this cell line, not only because the liver is the primary target organ for usnic acid's toxicity (Guo et al. 2008), but also the feasibility and capability of HepG2 cells for genetic modifications (silencing genes of interest in this study) enabled

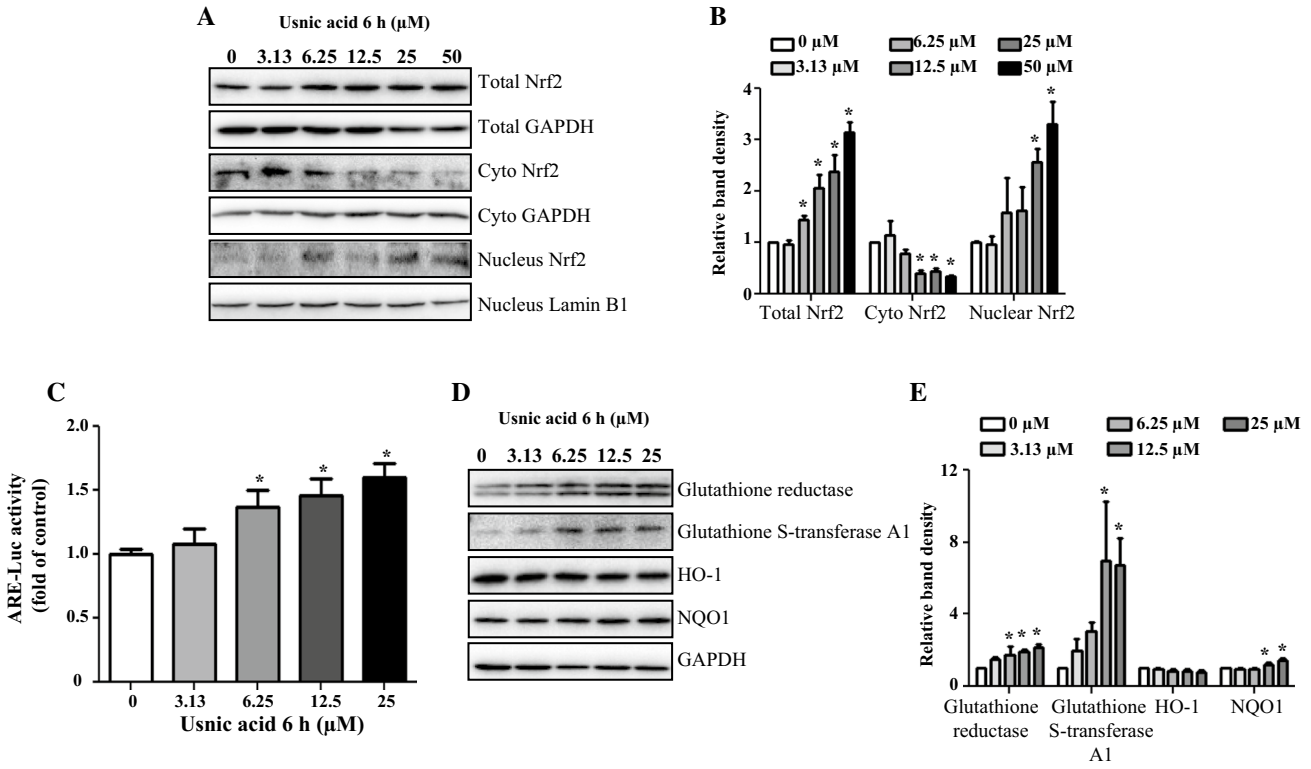

Fig. 6 Short-term treatment with usnic acid activates Nrf2-antioxidant response element signaling pathway in HepG2 cells. **a**, **b** Total cellular protein, cytoplasmic and nuclear protein fractions were extracted at 6 h after usnic acid treated, and expression levels of Nrf2 were detected by Western blotting. GAPDH was used as a loading control for total and cytosolic protein fraction, while lamin B1 was used as a loading control for the nuclear protein fractions. Intensities of bands for Nrf2 were normalized to the amount of GAPDH or lamin B1. *Bar graphs* show mean ± SD of three individual experiments. *$p < 0.05$ compared with DMSO vehicle control. **c** HepG2 cells were transfected with the luciferase reporter gene and ARE promoter region and then treated with different concentrations of usnic acid for 6 h. *Firefly* and *Renilla* luciferase activities were determined using a Dual-Luciferase® Reporter Assay System. The *bar graphs* show the mean ± SD of three experiments. *$p < 0.05$ versus treatment with DMSO vehicle control. **d**, **e** Western blotting was performed using antibodies for glutathione reductase, glutathione S-transferase, HO-1, NQO1, and GAPDH. Intensities of bands were normalized to the amount of GAPDH. *Bar graphs* are mean ± SD of three individual experiments. *$p < 0.05$ compared with DMSO vehicle control

us to elucidate in-depth molecular mechanisms (Chen et al. 2014a). As we previously discussed, we are aware that the activities of some drug metabolizing enzymes are lower in HepG2 cells than that in primary human hepatocytes and it may not be the best suited for metabolism-related toxicity study (Guo et al. 2011; Ning et al. 2008). However, metabolism was not the major focus of the present study because the parental form of usnic acid was shown to be more toxic to hepatocytes than its metabolites (Shi et al. 2014). It is worth noting that the human plasma concentration after intake of usnic acid remains unclear because it was marketed as dietary supplement and did not require clinical studies for regulatory approval. The calculated plasma concentration of usnic acid is 7.4–37 μM (Chen et al. 2014a) based on the recommended daily dose of 100–500 mg (Durazo et al. 2004; Favreau et al. 2002). The concentration of 3.13–50 μM used in this study falls in the range of plasma concentration and thus is clinically relevant.

Previous studies have investigated the DNA damaging effects of usnic acid in various biological systems. For instance, a study demonstrated that usnic acid induced DNA damage in Chinese hamster lung fibroblast V79 cells when measured using the comet assay (Leandro et al. 2013). Another study reported that the number of micronuclei was higher in usnic acid-treated human lymphocytes compared to those of the control group (Koparal et al. 2006). These data suggest that replication stress may contribute to usnic acid-associated toxicity. Whether or not usnic acid induces DNA damage in hepatic cells remained unclear, although there was an indication that usnic acid might be a DNA damaging agent since the DNA damage and repair associated gene UGT1A4 was induced when exposing usnic acid to HepG2 cells (Sahu et al. 2012). Cell cycle arrest at S phase in association with chemical-induced DNA damage also has been reported (Yang et al. 2014; Ye et al. 2003; Zhang et al. 2008), and interestingly, S-phase

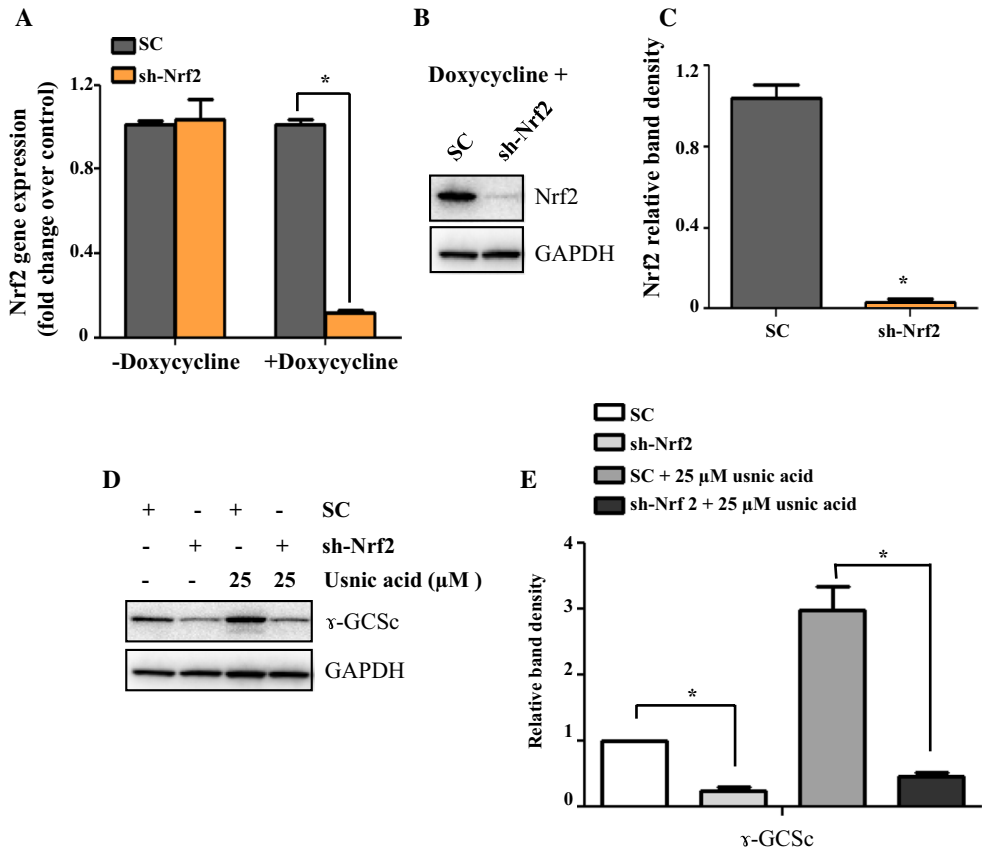

Fig. 7 Silencing of Nrf2 decreases usnic acid-induced γ-GCSc upregulation. HepG2 cells stably infected with lentivirus carrying doxycycline-inducible sh-Nrf2 or SC (scramble control). The two established cell lines were incubated with 1 μg/ml doxycycline for 72 h followed by continued culture for another 24 h without doxycycline; then, the efficiency of Nrf2 knockdown was determined by real-time PCR (**a**) and Western blotting (**b**, **c**). *Bar graphs* are mean ± SD of three individual experiments. *$p < 0.05$ compared with SC. **d**, **e** sh-Nrf2 and SC cells were incubated with doxycycline for 72 h and then treated with 25 μM usnic acid or DMSO vehicle control for another 24 h without doxycycline. Total protein were then isolated from treated cells. The expression levels of Nrf2, γ-GCSc, and GAPDH were detected by Western blot analyses. Intensities of bands were normalized to the amount of GAPDH. *Bar graphs* are mean ± SD of three individual experiments. *$p < 0.05$ compared with the SCs

arrest was observed in usnic acid-treated HepG2 cells in our previous study (Chen et al. 2014a). Studies, including ours, indicate that usnic acid causes mitochondrial dysfunction and ER stress (Chen et al. 2015; Han et al. 2004). It is known that mitochondria and endoplasmic reticulum (ER) are the major sites of cellular ROS generation. Thus, it is reasonable to anticipate that DNA could be damaged by usnic acid. As expected, a concentration-dependent elevation of DNA tail intensity in the comet assay and induction of γ-H2A.X, two characteristic indicators of DNA damage, were observed in this study (Fig. 3).

Pharmacologic studies have focused on usnic acid's antioxidant properties (de Paz et al. 2010; Odabasoglu et al. 2006). Usnic acid, like other antioxidants, also demonstrates pro-oxidative activity under certain conditions (Glebska et al. 2003; Guo et al. 2015). Polat et al. (2013) reported that usnic acid exhibits both antioxidative and pro-oxidative effects, depending on the concentrations tested. Recent evidence revealed that the generation of ROS and oxidative stress is associated with usnic acid's toxicity, and usnic acid has been recognized a pro-oxidant in these processes. For example, Han et al. (2004) reported that usnic acid triggered oxidative stress in primary cultured mouse hepatocytes, causing extensive liver toxicity. A gas chromatography–mass spectrometry-based metabolic profiling of the plasma and liver from usnic acid-treated rats showed that usnic acid disturbed energy and nucleotide metabolism and induced oxidative stress (Lu et al. 2011). An in vitro study using HepG2 cells demonstrated that usnic acid treatment increased the expression of biomarkers of oxidative stress (Sahu et al. 2012). Rabelo et al. (2012) conducted a study in SH-SY5Y neuronal-like cells and reported that usnic acid exhibited pro-oxidant properties which might be responsible for its neurotoxicological effect.

In good agreement with the results obtained from hepatic cells (Han et al. 2004; Sahu et al. 2012), we also

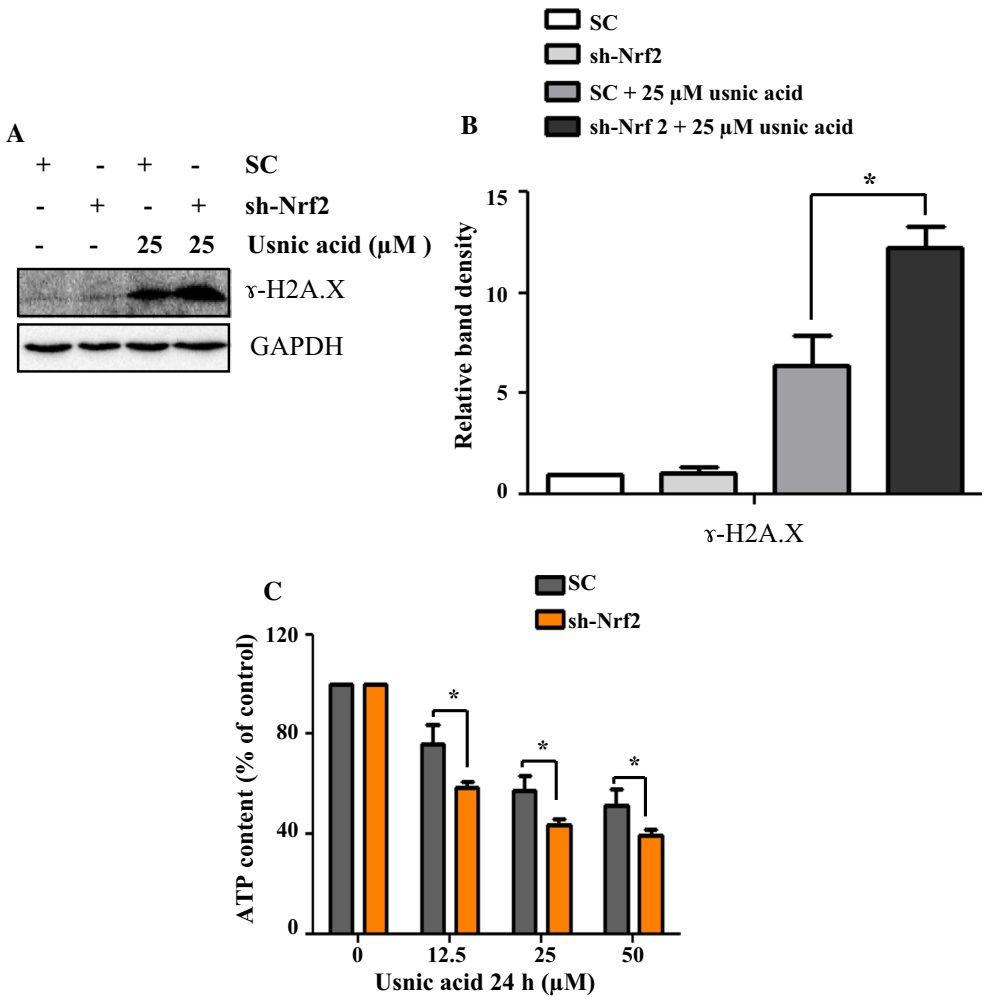

Fig. 8 Silencing of Nrf2 enhances usnic acid-induced DNA damage and decreases cell viability in HepG2 cells. sh-Nrf2 and SC cells were incubated with doxycycline for 72 h and then treated with 25 μM usnic acid or DMSO vehicle control for another 24 h without doxycycline. **a**, **b** The expression levels of γ-H2A.X and GAPDH were detected by Western blotting. Intensities of bands of γ-H2A.X were normalized to the amount of GAPDH. *Bar graphs* are mean ± SD of three individual experiments. *$p < 0.05$ sh-Nrf2 compared with the SC. **c** Cell viability was assessed by ATP assay. *Bar graphs* show the mean ± SD of three individual experiments. *$p < 0.05$ sh-Nrf2 versus the SCs

found that ROS production was increased time and concentration dependently (Fig. 4), which was accompanied by depletion of glutathione (Fig. 5). Oxidative stress is one of the consequences of the depletion of glutathione (GSH), while glutathione depletion has been demonstrated to be an important mechanism of liver toxicity caused by drugs, including the well-known liver toxicant acetaminophen (Hinson et al. 2010). In our study, glutathione depletion was also observed (Fig. 5a). *N*-acetyl-L-cysteine (NAC), an effective precursor of cysteine for glutathione synthesis to maintain cellular glutathione status and to protect cells from oxidative stress, was able to attenuate the cytotoxicity induced by usnic acid (Fig. 5f). These results indicate that usnic acid-induced oxidative stress is likely initiated by glutathione depletion. Although the precise mechanisms of glutathione depletion remain unclear, one possible mechanism may be worth further investigation, i.e., whether or not usnic acid is a substrate of glutathione transferase and can be metabolized via glutathionylation, resulting in glutathione depletion.

ROS plays important roles in regulating cell survival and death. Under normal physiologic conditions, cells maintain redox homeostasis through generation and elimination of ROS. In response to ROS, several lines of defensive signaling pathways are activated for cells to adapt and survive oxidative stress. These adaptive responses include the activation of redox-sensitive transcription factors, such as NF-kB, Ap-1 and Nrf2, and the activation of signal-transduction pathways, such as MAPK and PI3 K/Akt (Trachootham et al. 2008). Of these adaptive responses,

the well-studied Nrf2–ARE signaling pathway is the major survival mechanism in cells that provides defensive responses against oxidative stress and that regulates the expression of genes serving as ROS scavengers (Nguyen et al. 2009). Under unstressed conditions, cells maintain the Nrf2 protein at a low level by constant Nrf2 degradation via the ubiquitin–proteasome system. The primary regulator of Nrf2 ubiquitination is Kelch-like ECH-associated protein 1 (Keap1). Keap1 is an adaptor protein of cullin 3 and helps cullin 3 ubiquitinate Nrf2 via its E3 ubiquitin ligase complex (Kobayashi et al. 2004; Zhang et al. 2004). Upon excessive generation of ROS, the cysteine residues of Keap1 sense the intracellular insults and then Keap1 inhibits ubiquitin ligase activity by cullin 3, resulting in impaired ubiquitination of Nrf2, and thus, Nrf2 protein levels increase (Baird et al. 2013). When there is no longer sufficient Keap1 to maintain the suppression of Nrf2 protein, free cytosolic Nrf2 will translocate into the nucleus to transactivate its target genes (Harder et al. 2015). In our study, a marked increase in total Nrf2 protein was observed, indicating an accumulation of synthesized Nrf2 (Fig. 6a, b). Following the nuclear translocation of Nrf2, which was evidenced by profound increase in nuclear Nrf2, transcriptional regulation was activated as indicated by increased ARE-luciferase reporter activity and enhanced expression of Nrf2 target molecules in response to usnic acid treatment (Fig. 6c, d).

ROS plays a vital role in the initiation and progression of liver pathologies including those caused by alcohol, hepatic viruses, and drugs (Cederbaum et al. 2009; Jaeschke et al. 2002; Lu et al. 2013); however, the direct role of Nrf2 in liver toxicity, particularly in drug-induced liver toxicity, has not been well studied. In our study, taking advantage of the HepG2 hepatic cell line in which strategic genetic modifications can be performed more easily, we silenced the Nrf2 gene. In agreement with the outcome of Nrf2 knockdown mice, in which expression of Nrf2–ARE-regulated genes was downregulated (Chan et al. 2001; Enomoto et al. 2001), we found the expression of the Nrf2–ARE-regulated gene γ-GCSc was significantly downregulated when Nrf2 was silenced (Fig. 7d, e). Importantly, the silencing Nrf2 aggravated the toxic effects of usnic acid, such as DNA damage, as indicated by the augmentation of usnic acid-induced γ-H2A.X and cell death associated with ATP depletion (Fig. 8).

In summary, both our gene expression and biochemical studies in HepG2 cells demonstrated that usnic acid triggers oxidative stress and DNA damage. We found that Nrf2-mediated antioxidant responses are critical for usnic acid-induced DNA damage and that silencing Nrf2 increases the susceptibility of HepG2 cells to usnic acid-associated cytotoxicity. Our study not only elucidates the direct role of the Nrf2 signaling pathway in usnic acid-induced liver toxicity but also highlights the significance of monitoring Nrf2 activity in chemical- or drug-induced liver toxicity, especially at earlier time points prior to the onset cellular damage.

Acknowledgments ZH. Z., DK. Y., and Z. R. were supported by appointments to the Postgraduate Research Program at the National Center for Toxicological Research administered by the Oak Ridge Institute for Science Education through an interagency agreement between the US Department of Energy and the U.S. FDA. This work was supported by U.S. FDA's intramural grant. L.S. was supported by the National High Technology Research and Development Program of China (2015AA020104), the National Natural Science Foundation of China (31471239), the 111 Project (B13016), and the National Supercomputer Center in Guangzhou, China

Compliance with ethical standards

Conflict of interest The authors declare that no conflict of interest.

References

Alam J, Stewart D, Touchard C, Boinapally S, Choi AM, Cook JL (1999) Nrf2, a Cap'n'Collar transcription factor, regulates induction of the heme oxygenase-1 gene. J Biol Chem 274(37):26071–26078

Araujo AA, de Melo MG, Rabelo TK, Nunes PS, Santos SL, Serafini MR, Santos MR, Quintans-Junior LJ, Gelain DP (2015) Review of the biological properties and toxicity of usnic acid. Nat Prod Res 29(23):2167–2180

Baird L, Lleres D, Swift S, Dinkova-Kostova AT (2013) Regulatory flexibility in the Nrf2-mediated stress response is conferred by conformational cycling of the Keap1-Nrf2 protein complex. Proc Natl Acad Sci USA 110(38):15259–15264

Bell SP, Dutta A (2002) DNA replication in eukaryotic cells. Annu Rev Biochem 71:333–374

Bertoli C, Skotheim JM, de Bruin RA (2013) Control of cell cycle transcription during G1 and S phases. Nat Rev Mol Cell Biol 14(8):518–528

Bolger AM, Lohse M, Usadel B (2014) Trimmomatic: a flexible trimmer for Illumina sequence data. Bioinformatics 30(15):2114–2120

Bryan HK, Olayanju A, Goldring CE, Park BK (2013) The Nrf2 cell defence pathway: Keap1-dependent and -independent mechanisms of regulation. Biochem Pharmacol 85(6):705–717

Cederbaum AI, Lu Y, Wu D (2009) Role of oxidative stress in alcohol-induced liver injury. Arch Toxicol 83(6):519–548

CFSAN (2001) FDA warns consumers not to use the dietary supplement LipoKinetix. http://www.fdagov/safety/medwatch/safetyinformation/safetyalertsforhumanmedicalproducts/ucm-174455htm. Accessed 15 Dec 2015

Chan K, Han XD, Kan YW (2001) An important function of Nrf2 in combating oxidative stress: detoxification of acetaminophen. Proc Natl Acad Sci USA 98(8):4611–4616

Chen S, Dobrovolsky VN, Liu F, Wu Y, Zhang Z, Mei N, Guo L (2014a) The role of autophagy in usnic acid-induced toxicity in hepatic cells. Toxicol Sci 142(1):33–44

Chen S, Xuan J, Couch L, Iyer A, Wu Y, Li QZ, Guo L (2014b) Sertraline induces endoplasmic reticulum stress in hepatic cells. Toxicology 322:78–88

Chen S, Zhang Z, Wu Y, Shi Q, Yan H, Mei N, Tolleson WH, Guo L (2015) Endoplasmic reticulum stress and store-operated calcium entry contribute to usnic acid-induced toxicity in hepatic cells. Toxicol Sci 146(1):116–126

de Paz GA, Raggio J, Gomez-Serranillos MP, Palomino OM, Gonzalez-Burgos E, Carretero ME, Crespo A (2010) HPLC isolation of antioxidant constituents from Xanthoparmelia spp. J Pharm Biomed Anal 53(2):165–171

Devasagayam TP, Tilak JC, Boloor KK, Sane KS, Ghaskadbi SS, Lele RD (2004) Free radicals and antioxidants in human health: current status and future prospects. J Assoc Phys India 52:794–804

Doi H, Iwasaki H, Masubuchi Y, Nishigaki R, Horie T (2002) Chemiluminescence associated with the oxidative metabolism of salicylic acid in rat liver microsomes. Chem Biol Interact 140(2):109–119

Durazo FA, Lassman C, Han SH, Saab S, Lee NP, Kawano M, Saggi B, Gordon S, Farmer DG, Yersiz H, Goldstein RL, Ghobrial M, Busuttil RW (2004) Fulminant liver failure due to usnic acid for weight loss. Am J Gastroenterol 99(5):950–952

Enomoto A, Itoh K, Nagayoshi E, Haruta J, Kimura T, O'Connor T, Harada T, Yamamoto M (2001) High sensitivity of Nrf2 knockout mice to acetaminophen hepatotoxicity associated with decreased expression of ARE-regulated drug metabolizing enzymes and antioxidant genes. Toxicol Sci 59(1):169–177

Evans MD, Cooke MS (2004) Factors contributing to the outcome of oxidative damage to nucleic acids. BioEssays 26(5):533–542

Favreau JT, Ryu ML, Braunstein G, Orshansky G, Park SS, Coody GL, Love LA, Fong TL (2002) Severe hepatotoxicity associated with the dietary supplement LipoKinetix. Ann Intern Med 136(8):590–595

Glebska J, Skolimowski J, Kudzin Z, Gwozdzinski K, Grzelak A, Bartosz G (2003) Pro-oxidative activity of nitroxides in their reactions with glutathione. Free Radic Biol Med 35(3):310–316

Gold R, Kappos L, Arnold DL, Bar-Or A, Giovannoni G, Selmaj K, Tornatore C, Sweetser MT, Yang M, Sheikh SI, Dawson KT, Investigators DS (2012) Placebo-controlled phase 3 study of oral BG-12 for relapsing multiple sclerosis. N Engl J Med 367(12):1098–1107

Guo L, Shi Q, Fang JL, Mei N, Ali AA, Lewis SM, Leakey JE, Frankos VH (2008) Review of usnic acid and Usnea barbata toxicity. J Environ Sci Health C Environ Carcinog Ecotoxicol Rev 26(4):317–338

Guo L, Dial S, Shi L, Branham W, Liu J, Fang JL, Green B, Deng H, Kaput J, Ning B (2011) Similarities and differences in the expression of drug-metabolizing enzymes between human hepatic cell lines and primary human hepatocytes. Drug Metab Dispos 39(3):528–538

Guo X, Chen S, Zhang Z, Dobrovolsky VN, Dial SL, Guo L, Mei N (2015) Reactive oxygen species and c-Jun N-terminal kinases contribute to TEMPO-induced apoptosis in L5178Y cells. Chem Biol Interact 235:27–36

Han D, Matsumaru K, Rettori D, Kaplowitz N (2004) Usnic acid-induced necrosis of cultured mouse hepatocytes: inhibition of mitochondrial function and oxidative stress. Biochem Pharmacol 67(3):439–451

Harder B, Jiang T, Wu T, Tao S, de la Vega MR, Tian W, Chapman E, Zhang DD (2015) Molecular mechanisms of Nrf2 regulation and how these influence chemical modulation for disease intervention. Biochem Soc Trans 43(4):680–686

Hayes JD, Chanas SA, Henderson CJ, McMahon M, Sun C, Moffat GJ, Wolf CR, Yamamoto M (2000) The Nrf2 transcription factor contributes both to the basal expression of glutathione S-transferases in mouse liver and to their induction by the chemopreventive synthetic antioxidants, butylated hydroxyanisole and ethoxyquin. Biochem Soc Trans 28(2):33–41

Hinson JA, Roberts DW, James LP (2010) Mechanisms of acetaminophen-induced liver necrosis. Handb Exp Pharmacol 196:369–405

Itoh K, Chiba T, Takahashi S, Ishii T, Igarashi K, Katoh Y, Oyake T, Hayashi N, Satoh K, Hatayama I, Yamamoto M, Nabeshima Y (1997) An Nrf2/small Maf heterodimer mediates the induction of phase II detoxifying enzyme genes through antioxidant response elements. Biochem Biophys Res Commun 236(2):313–322

Jaeschke H, Gores GJ, Cederbaum AI, Hinson JA, Pessayre D, Lemasters JJ (2002) Mechanisms of hepatotoxicity. Toxicol Sci 65(2):166–176

Kobayashi A, Kang MI, Okawa H, Ohtsuji M, Zenke Y, Chiba T, Igarashi K, Yamamoto M (2004) Oxidative stress sensor Keap1 functions as an adaptor for Cul3-based E3 ligase to regulate proteasomal degradation of Nrf2. Mol Cell Biol 24(16):7130–7139

Koparal AT, Tuylu BA, Turk H (2006) In vitro cytotoxic activities of (+)-usnic acid and (−)-usnic acid on V79, A549, and human lymphocyte cells and their non-genotoxicity on human lymphocytes. Nat Prod Res 20(14):1300–1307

Leandro LF, Munari CC, Sato VL, Alves JM, de Oliveira PF, Mastrocola DF, Martins Sde P, Moraes Tda S, de Oliveira AI, Tozatti MG, Cunha WR, Tavares DC (2013) Assessment of the genotoxicity and antigenotoxicity of (+)-usnic acid in V79 cells and Swiss mice by the micronucleus and comet assays. Mutat Res 753(2):101–106

Lu X, Zhao Q, Tian Y, Xiao S, Jin T, Fan X (2011) A metabonomic characterization of (+)-usnic acid-induced liver injury by gas chromatography-mass spectrometry-based metabolic profiling of the plasma and liver in rat. Int J Toxicol 30(5):478–491

Lu J, Miyakawa K, Roth RA, Ganey PE (2013) Tumor necrosis factor-alpha potentiates the cytotoxicity of amiodarone in Hepa1c1c7 cells: roles of caspase activation and oxidative stress. Toxicol Sci 131(1):164–178

Martindale JL, Holbrook NJ (2002) Cellular response to oxidative stress: signaling for suicide and survival. J Cell Physiol 192(1):1–15

Neff GW, Reddy KR, Durazo FA, Meyer D, Marrero R, Kaplowitz N (2004) Severe hepatotoxicity associated with the use of weight loss diet supplements containing ma huang or usnic acid. J Hepatol 41(6):1062–1064

Nguyen T, Nioi P, Pickett CB (2009) The Nrf2-antioxidant response element signaling pathway and its activation by oxidative stress. J Biol Chem 284(20):13291–13295

Ning B, Dial S, Sun Y, Wang J, Yang J, Guo L (2008) Systematic and simultaneous gene profiling of 84 drug-metabolizing genes in primary human hepatocytes. J Biomol Screen 13(3):194–201

Odabasoglu F, Cakir A, Suleyman H, Aslan A, Bayir Y, Halici M, Kazaz C (2006) Gastroprotective and antioxidant effects of usnic acid on indomethacin-induced gastric ulcer in rats. J Ethnopharmacol 103(1):59–65

Ozben T (2007) Oxidative stress and apoptosis: impact on cancer therapy. J Pharm Sci 96(9):2181–2196

Polat Z, Aydin E, Turkez H, Aslan A (2016) In vitro risk assessment of usnic acid compound. Toxicol Ind Health 32(3):468–475

Rabelo TK, Zeidan-Chulia F, Vasques LM, dos Santos JP, da Rocha RF, Pasquali MA, Rybarczyk-Filho JL, Araujo AA, Moreira JC, Gelain DP (2012) Redox characterization of usnic acid and its cytotoxic effect on human neuron-like cells (SH-SY5Y). Toxicol In Vitro 26(2):304–314

Ravanat JL, Martinez GR, Medeiros MH, Di Mascio P, Cadet J (2004) Mechanistic aspects of the oxidation of DNA constituents mediated by singlet molecular oxygen. Arch Biochem Biophys 423(1):23–30

Rogakou EP, Pilch DR, Orr AH, Ivanova VS, Bonner WM (1998) DNA double-stranded breaks induce histone H2AX phosphorylation on serine 139. J Biol Chem 273(10):5858–5868

Sahu SC, Amankwa-Sakyi M, O'Donnell MW Jr, Sprando RL (2012) Effects of usnic acid exposure on human hepatoblastoma HepG2 cells in culture. J Appl Toxicol 32(9):722–730

Shackelford RE, Kaufmann WK, Paules RS (2000) Oxidative stress and cell cycle checkpoint function. Free Radic Biol Med 28(9):1387–1404

Shi Q, Greenhaw J, Salminen WF (2014) Inhibition of cytochrome P450s enhances (+)-usnic acid cytotoxicity in primary cultured rat hepatocytes. J Appl Toxicol 34(8):835–840

Sies H (1997) Oxidative stress: oxidants and antioxidants. Exp Physiol 82(2):291–295

Solis WA, Dalton TP, Dieter MZ, Freshwater S, Harrer JM, He L, Shertzer HG, Nebert DW (2002) Glutamate-cysteine ligase modifier subunit: mouse Gclm gene structure and regulation by agents that cause oxidative stress. Biochem Pharmacol 63(9):1739–1754

Thimmulappa RK, Mai KH, Srisuma S, Kensler TW, Yamamoto M, Biswal S (2002) Identification of Nrf2-regulated genes induced by the chemopreventive agent sulforaphane by oligonucleotide microarray. Cancer Res 62(18):5196–5203

Trachootham D, Lu W, Ogasawara MA, Nilsa RD, Huang P (2008) Redox regulation of cell survival. Antioxid Redox Signal 10(8):1343–1374

Trapnell C, Roberts A, Goff L, Pertea G, Kim D, Kelley DR, Pimentel H, Salzberg SL, Rinn JL, Pachter L (2012) Differential gene and transcript expression analysis of RNA-seq experiments with TopHat and Cufflinks. Nat Protoc 7(3):562–578

Venugopal R, Jaiswal AK (1996) Nrf1 and Nrf2 positively and c-Fos and Fra1 negatively regulate the human antioxidant response element-mediated expression of NAD(P)H:quinone oxidoreductase1 gene. Proc Natl Acad Sci USA 93(25):14960–14965

Vertuani S, Angusti A, Manfredini S (2004) The antioxidants and pro-antioxidants network: an overview. Curr Pharm Des 10(14):1677–1694

Yang Q, He X, Li X, Xu W, Luo Y, Yang X, Wang Y, Li Y, Huang K (2014) DNA damage and S phase arrest induced by Ochratoxin A in human embryonic kidney cells (HEK 293). Mutat Res 765:22–31

Ye X, Franco AA, Santos H, Nelson DM, Kaufman PD, Adams PD (2003) Defective S phase chromatin assembly causes DNA damage, activation of the S phase checkpoint, and S phase arrest. Mol Cell 11(2):341–351

Yellapu RK, Mittal V, Grewal P, Fiel M, Schiano T (2011) Acute liver failure caused by 'fat burners' and dietary supplements: a case report and literature review. Can J Gastroenterol 25(3):157–160

Zhang DD, Lo SC, Cross JV, Templeton DJ, Hannink M (2004) Keap1 is a redox-regulated substrate adaptor protein for a Cul3-dependent ubiquitin ligase complex. Mol Cell Biol 24(24):10941–10953

Zhang WH, Poh A, Fanous AA, Eastman A (2008) DNA damage-induced S phase arrest in human breast cancer depends on Chk1, but G(2) arrest can occur independently of Chk1, Chk2 or MAPKAPK2. Cell Cycle 7(11):1668–1677

Zhang Z, Chen S, Mei H, Xuan J, Guo X, Couch L, Dobrovolsky VN, Guo L, Mei N (2015) Ginkgo biloba leaf extract induces DNA damage by inhibiting topoisomerase II activity in human hepatic cells. Sci Rep 5:14633